

Dark Matter And $B_s \rightarrow \mu^+ \mu^-$ With Minimal SO_{10} Soft SUSY Breaking

Radovan Dermisek

Davis Institute for High Energy Physics,
University of California, Davis, CA 95616, USA
E-mail: dermisek@physics.ucdavis.edu

Stuart Raby

Department of Physics, The Ohio State University,
174 W. 18th Ave., Columbus, Ohio 43210, USA ;
On leave of absence, School of Natural Sciences,
Institute for Advanced Study, Princeton, NJ 08540, USA
E-mail: raby@pacific.mps.ohio-state.edu

Leszek Roszkowski

Department of Physics, Lancaster University, Lancaster LA1 4YB, England
E-mail: L.Roszkowski@lancaster.ac.uk

Roberto Ruiz de Austri

Physics Division, School of Technology, Aristotle University of Thessaloniki,
GR - 540 06 Thessaloniki, Greece
E-mail: rruiz@gen.auth.gr

Abstract: CMSSM boundary conditions are usually used when calculating cosmological dark matter densities. In this paper we calculate the cosmological density of dark matter in the MSSM using minimal SO_{10} soft SUSY breaking boundary conditions. These boundary conditions incorporate several attractive features: they are consistent with SO_{10} Yukawa unification, they result in a "natural" inverted scalar mass hierarchy and they reduce the dimension 5 operator contribution to the proton decay rate. With regards to dark matter, on the other hand, this is to a large extent an unexplored territory with large squark and slepton masses m_{16} , large A_0 and small $f; M_{1=2}g$. We find that in most regions of parameter space the cosmological density of dark matter is considerably less than required by the data. However there is a well defined, narrow region of parameter space which provides the observed relic density of dark matter, as well as a good fit to precision electroweak data, including top, bottom and tau masses, and acceptable bounds on the branching fraction of $B_s \rightarrow \mu^+ \mu^-$. We present predictions for Higgs and SUSY spectra, the dark matter detection cross section and the branching ratio $BR(B_s \rightarrow \mu^+ \mu^-)$ in this region of parameter space.

Keyw ords: Supersym m etric E ective Theories, Cosm ology of Theories beyond the SM , Dark M atter.

Contents

1. Introduction	1
2. Minimal SO_{10} SUSY Model { $MSO_{10}SM$	2
2.1 Framework	2
2.2 Analysis	4
3. Cosmological Dark Matter Density	5
4. Predictions and Summary	11

1. Introduction

The constrained minimal supersymmetric standard model [CMSSM] [1] is a well defined model for soft SUSY breaking with five independent parameters given by m_0 ; $M_{1=2}$; A_0 ; $\tan\beta$ and $\text{sign}(\mu)$. It has been used extensively for benchmark points for collider searches, as well as for astrophysical and dark matter analyses. The economy of parameters in this scheme makes it a useful tool for exploring SUSY phenomena. However the CMSSM may miss regions of soft SUSY breaking parameter space which give qualitatively different predictions. In this paper we consider an alternate scheme, the minimal SO_{10} supersymmetric model [MSO₁₀SM], which is well motivated and opens up a qualitatively new region of parameter space.

In the MSO₁₀SM there are 7 soft SUSY breaking parameters m_0 ; $M_{1=2}$; A_0 ; $\tan\beta$, m_{16} (a universal squark and slepton mass), m_{10} (a universal Higgs mass) and m_H^2 (Higgs up/down mass splitting). Moreover the parameters A_0 ; m_{10} ; m_{16} must satisfy the constraints [2, 3, 4] $A_0 \leq 2m_{16}$, $m_{10} \leq \sqrt{2}m_{16}$, $m_{16} > 1.2 \text{ TeV}$ with $\tan\beta \leq 50$; $M_{1=2} \leq m_{16}$ and $\tan\beta \leq 50$. Note, with these values of the soft SUSY breaking parameters, we can explore SUSY phenomena with qualitatively different behavior than in the CMSSM. This is mainly due to the Higgs splitting (m_H^2) which, as is well known [5], enables one to obtain electroweak symmetry breaking with values $m_{16} \leq m_{1=2}$; $M_{1=2} \leq m_{16}$. Also, radiative EW SB with $\tan\beta \leq 50$ requires significantly less fine tuning with Higgs mass splitting (see Rattazzi and Sarid [5]). Furthermore, with 3 Higgs mass parameters m_{10} ; m_{16} ; and m_H^2 we find that the latter two are strongly constrained by EW SB, once we fix the value of m_{10} , which we treat as a free parameter. This is unlike the CMSSM where m_{10} is fixed by EW SB. Also note that small changes in m_H^2 lead to big changes in the CP odd Higgs mass m_A [2].

It is not at all obvious that the MSO₁₀SM region of soft SUSY breaking parameter space is consistent with cosmology [3, 4]. The dark matter candidate in this model is the lightest neutralino. However, since the scalar masses of the first two families are of order

$m_{16} > 1.2 \text{ TeV}$, and the third generation sfermions (except for the stops) also tend to be heavy, the usually dominant annihilation channels, for the neutralino LSP to light fermions via t-channel sfermion exchange, are suppressed. On the other hand, the process $\tilde{\chi}_1^0 \rightarrow f\bar{f}$ via s-channel A exchange becomes important. This is due to the enhanced CP odd Higgs coupling to down-type fermions, which is proportional to $\tan\beta$, and because, in contrast to heavy scalar exchange, the process is not p-wave suppressed. In an earlier analysis, our χ^2 analysis favored a light CP odd Higgs mass $m_A \approx 100 \text{ GeV}$ [2], although heavier A were also allowed. Such light A are however disfavored for two reasons. In order to provide efficient annihilation for the LSPs, one would be squeezed into a rather low LSP mass region $m_{\tilde{\chi}_1^0} = m_A = 2$, which would require extreme fine-tuning at best. In addition, such low m_A are anyway inconsistent with the current limits on $\text{BR}(\tilde{B}_s \rightarrow \tilde{\chi}_1^0 + \dots)$. In this analysis, we vary the A mass.

We study the cosmology of the MSO_{10}SM in this paper. Obtaining the observed relic abundance of cold dark matter, which along with other cosmological parameters has recently been determined with an unprecedented accuracy [6], will provide a new important constraint on the model. We also compute the branching ratio for the process $\tilde{B}_s \rightarrow \tilde{\chi}_1^0 + \dots$ due to A exchange [7]. It is absolutely essential to include this latter constraint in our analysis. Note, the CDF bound $\text{BR}(\tilde{B}_s \rightarrow \tilde{\chi}_1^0 + \dots) < 2.6 \times 10^{-6}$ [8]. The cross section for the direct detection of dark matter is also computed. In section 2 we define the MSO_{10}SM , describe its virtues and outline the analysis. In section 3 we compute the cosmological dark matter density and discuss our results. Then in section 4 we discuss our predictions for underground dark matter searches and for collider Higgs and SUSY searches.

2. Minimal SO_{10} SUSY Model { MSO_{10}SM

2.1 Framework

Let us define the minimal SO_{10} SUSY model. Quarks and leptons of one family reside in the 16 dimensional representation, while the two Higgs doublets of the MSSM reside in one 10 dimensional representation. For the third generation we assume the minimal Yukawa coupling term given by

$$16 \otimes 10 \otimes 16: \tag{2.1}$$

On the other hand, for the first two generations and for their mixing with the third, we assume a hierarchical mass matrix structure due to effective higher dimensional operators. Hence the third generation Yukawa couplings satisfy $t = b = \dots = \dots$.

Soft SUSY breaking parameters are also consistent with SO_{10} with

a universal gaugino mass $M_{1=2}$,

a universal squark and slepton mass m_{16}^1 ,

a universal scalar Higgs mass m_{10} ,

¹ SO_{10} does not require all sfermions to have the same mass. This however may be enforced by non-abelian family symmetries or possibly by the SUSY breaking mechanism.

and a universal A parameter A_0 .

In addition we have the soft SUSY breaking Higgs mass parameters m_{10} and m_{16} . m_{10} may, as in the CMSSM, be exchanged for $\tan\beta$. Note, not all of these parameters are independent. Indeed, in order to fit the low energy electroweak data, including the third generation fermion masses, it has been shown that $A_0; m_{10}; m_{16}$ must satisfy the constraints [2]

$$\begin{aligned} A_0 &= \frac{2m_{16}}{m_{10}} \\ m_{10} &> 1.2 \text{ TeV} \\ &; M_{1=2} = m_{16} \end{aligned} \quad (2.2)$$

with

$$\tan\beta = 50 \quad (2.3)$$

This result has been confirmed in two recent analyses [3, 4]. The first property (Eqn. (2.2)) is necessary to fit the top, bottom and τ masses, in addition to the precision electroweak data [2, 3, 4]. The second property (Eqn. (2.3)) is a consequence of third generation Yukawa unification, since $m_t(m_t) = m_b(m_t) \tan\beta$.

One loop threshold corrections at the GUT scale lead to two significant parameters we treat as free parameters, although they are calculable in any GUT. The first is a correction to gauge coupling unification given by

$$\alpha_3(M_G) = \alpha_G \quad (2.4)$$

where the GUT scale M_G is defined as the scale where $\alpha_1(M_G) = \alpha_2(M_G) = \alpha_G$. The second is a Higgs splitting mass parameter defined by

$$m_H^2 = (m_{H_d}^2 - m_{H_u}^2) = 2m_{10}^2 \quad (2.5)$$

In order to fit the low energy data we find $\alpha_3 = 4\%$ and $m_H^2 = 13\%$ [2]. The largest corrections to α_3 come from the Higgs and SO_{10} breaking sectors, while the correction to m_H^2 is predominantly due to the right-handed neutrino. For $M = 10^{13-14}$ GeV (appropriate for a light neutrino mass 0.06 eV) we obtain $m_H^2 = 10-7\%$.

Finally, as a bonus, these same values of soft SUSY breaking parameters, with $m_{16} = 1.2$ TeV, result in two very interesting consequences. Firstly, it "naturally" produces an inverted scalar mass hierarchy [ISMH] [9]. With an ISMH squarks and sleptons of the first two generations obtain mass of order m_{16} at M_Z . The stop, sbottom, and stau, on the other hand, have mass less than a TeV. An ISMH has two virtues.

1. It preserves "naturalness" (for values of m_{16} which are not too large), since only the third generation squarks and sleptons couple strongly to the Higgs.
2. It ameliorates the SUSY CP and flavor problems, since these constraints on CP violating angles or flavor violating squark and slepton masses are strongest for the first two generations, yet they are suppressed as $1/m_{16}^2$. For $m_{16} > \text{a few TeV}$, these constraints are weakened [10].

Secondly, Super{Kamionokande bounds on $(p \rightarrow K^+ \gamma) > 1:9 \cdot 10^{13}$ yrs. [11] constrain the contribution of dimension 5 baryon and lepton number violating operators. These are however minimized with $\mu; M_{1=2}; m_{16}$ [12].

2.2 Analysis

We use a top{down approach with a global χ^2 analysis [13]. The input parameters are defined by boundary conditions at the GUT scale. The 11 input parameters at M_G are given by $|$ three gauge parameters $M_G; g_3; g_2; g_1$; the Yukawa coupling y_t , and 7 soft SUSY breaking parameters $\mu; M_{1=2}; A_0; \tan \beta, m_{16}^2; m_{10}^2; m_H^2$. These are fit in a global χ^2 analysis defined in terms of physical low energy observables. Note we keep three parameters $(m_{16}; \mu; M_{1=2})$ fixed; while minimizing χ^2 with the remaining 8 parameters. Below we will plot χ^2 contours as a function of $\mu; M_{1=2}$ for different values of m_{16} . We use two (one) loop renormalization group [RG] running for dimensionless (dimensionful) parameters from M_G to M_Z .² We require electroweak symmetry breaking using an improved Higgs potential, including m_t^4 and m_b^4 corrections in an effective 2 Higgs doublet model below $M_{SUSY} = \frac{1}{2}(m_{\tilde{t}_1}^2 + m_{\tilde{t}_2}^2)$ [14].

The χ^2 function includes 9 observables; 6 precision electroweak data $\alpha_{EM}; G_F; s(M_Z); M_Z; M_W; n_{EW}$ and the 3 fermion masses $M_{top}; m_b(m_b); M_\tau$. In our analysis we fit the central values [15]: $M_Z = 91:188$ GeV, $M_W = 80:419$ GeV, $G_F = 1:1664$ GeV⁻², $\alpha_{EM}^{-1} = 137:04$; $M_\tau = 1:7770$ GeV with 0.1% numerical uncertainties; and the following with the experimental uncertainty in parentheses: $s(M_Z) = 0:1180$ (0:0020); $n_{EW} = 10^3 = 0:200$ (1:1) [17], $M_\tau = 174:3$ (5:1) GeV, $m_b(m_b) = 4:20$ (0:20) GeV.³ We include the complete one loop threshold corrections at M_Z to all observables. In addition we use one loop QED and three loop QCD RG running below M_Z .

The output of this analysis is a set of weak scale squark, slepton, gaugino and Higgs masses. With regards to the calculated Higgs and sparticle masses, the neutral Higgs masses $h; H; A$ are pole masses calculated with the leading top, bottom, stop, sbottom loop contributions; while all other sparticle masses are running masses. This output is then used to compute the cosmological dark matter density of the lightest neutralino which is the LSP. The dark matter analysis is discussed in more detail in section 3.

Using χ^2 penalties⁴ we apply two additional constraints:

$$m_{\tilde{t}_1} \leq 300 \text{ GeV}$$

$$m_A \text{ fixed.}$$

The first is chosen to be consistent with BR $(B \rightarrow X_s \gamma)$ [2]. Note, although we do calculate BR $(B \rightarrow X_s \gamma)$, we do not use it as a constraint in the analysis. This is for two

²Note, we have checked that switching to 2 loop RGEs for dimensionful parameters can be compensated for by small changes in the GUT scale parameters, without significant changes in the low energy results.

³Note we take a conservative error for $m_b(m_b)$ [15] in view of recent claim to much smaller errors [16].

⁴In order to constrain the values of some physical observables in our χ^2 analysis, such as $m_{\tilde{t}_1}$ or m_A , we add a significant contribution to the χ^2 function for values of these observables outside the desired range. We refer to this additional contribution as a χ^2 penalty. Minimization of χ^2 with Minuit, then pushes the fits to the desired range. Of course the χ^2 penalties then vanish.

reasons | 1) this decay mode depends on 3{2 generation mixing which is model dependent and 2) it is not difficult to get $\text{BR}(B \rightarrow X_s \gamma)$ for values of $m_{\tilde{t}_1} \approx 300$ GeV. Hence, in order to be generally consistent with the measured value of $\text{BR}(B \rightarrow X_s \gamma)$, we impose $m_{\tilde{t}_1} \approx 300$ GeV. With regards to the second constraint, since h^2 and $\text{BR}(B_s \rightarrow \mu^+ \mu^-)$ are both sensitive to the value of m_A , we fix its value and present our results for different values of m_A .⁵

Finally, we apply the experimental limits:

lower bound on the lightest chargino mass $m_{\tilde{\chi}_1^\pm} > 104$ GeV,

lower bound on the light Higgs mass $m_h > 111$ GeV.

Note, because of the theoretical uncertainty in the calculation of m_h (≈ 3 GeV), we conservatively impose $m_h > 111$ GeV, instead of the LEP bound for SM Higgs $m_h > 114.4$ GeV.

3. Cosmological Dark Matter Density

We compute the relic abundance h^2 of the lightest neutralino using exact expressions for neutralino pair annihilation into all allowed final state channels, which are valid both near and further away from resonances and thresholds [18]. We further treat the neutralino coannihilation with the lightest chargino and next-to-lightest neutralino [19] and with the lighter stau [20] with similar precision. We only neglect the neutralino coannihilation with the stop which would only affect h^2 in the regions of parameter space which are uninteresting for other reasons, as we comment below. We solve the Boltzmann equation numerically as in [21] and compute h^2 with an error of a few per cent, which is comparable with today's accuracy on the observational side. The latest determinations of cosmological parameters [6] give $\Omega_M h^2 = 0.135^{+0.008}_{-0.009}$ for the total matter content and $\Omega_b h^2 = 0.0224 \pm 0.0009$ for the baryonic component. The difference, attributed to cold dark matter (CDM), is then

$$\Omega_{\text{CDM}} h^2 = 0.113 \pm 0.009; \quad (3.1)$$

which is significantly narrower than previous ranges. We then apply two constraints on the dark matter abundance:

the upper bound $h^2 < 0.13$,

2) preferred range $0.095 < h^2 < 0.13$.

In Figs. 1{3 we present our results for different values of m_{16} and m_A in the (m_{16}, m_A) plane. In particular in Fig. 1 we present, for $m_{16} = 3$ TeV and $m_A = 500$ GeV, the (magenta) lines of constant h^2 with the cosmologically preferred dark matter region (shaded green) satisfying $0.095 < h^2 < 0.13$. We find significant regions of parameter space

⁵The calculation of $\text{BR}(B \rightarrow X_s \gamma)$ and $\text{BR}(B_s \rightarrow \mu^+ \mu^-)$ requires a model for fermion mass matrices. In the absence of such a model we use the observed CKM matrix elements to calculate these flavor violating branching ratios.

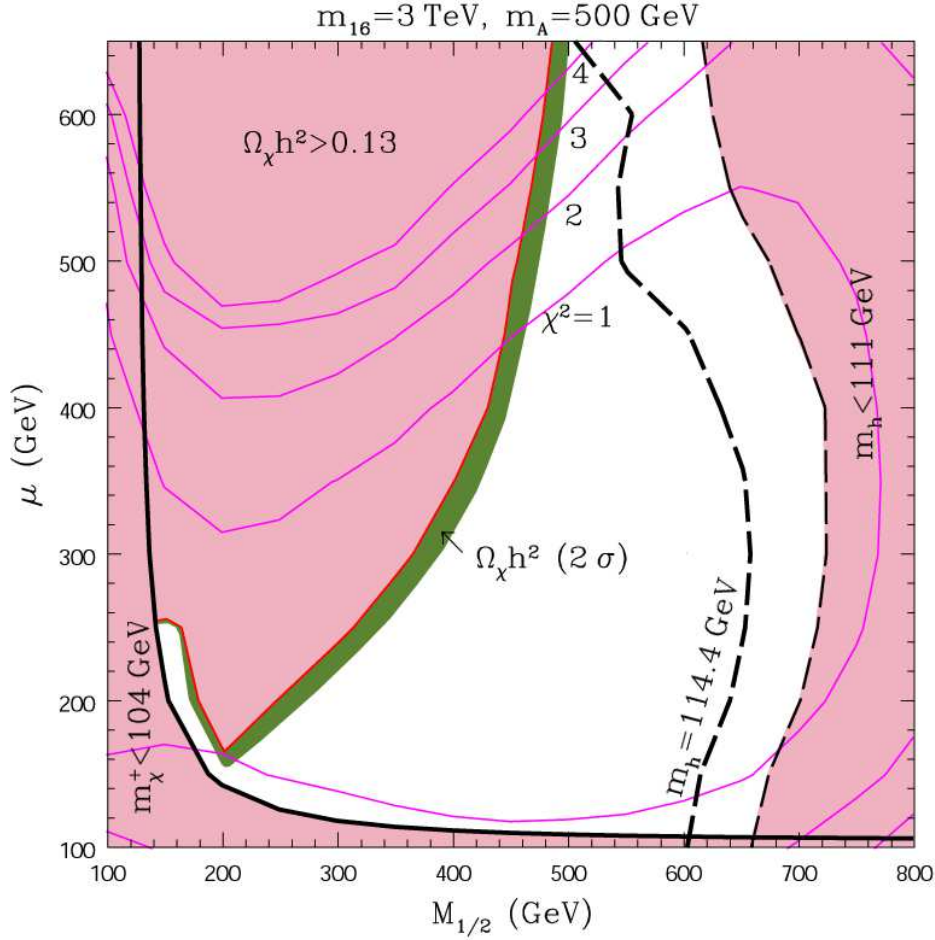


Figure 1: Contours of constant χ^2 for $m_{16} = 3 \text{ TeV}$ and $m_A = 500 \text{ GeV}$. The red regions are excluded by $m_{\tilde{\chi}^+} < 104 \text{ GeV}$ (below and to the left of a black solid curve), $m_h < 111 \text{ GeV}$ (on the right) and by $\Omega_{\tilde{\chi}} h^2 > 0.13$. To the right of the black broken line one has $m_h < 114.4 \text{ GeV}$. The green band corresponds to the preferred 2σ range $0.095 < \Omega_{\tilde{\chi}} h^2 < 0.13$, while the white regions below it correspond to $\Omega_{\tilde{\chi}} h^2 < 0.095$.

which gives $\Omega_{\tilde{\chi}} h^2 \approx 0.13$, $\Omega_{\tilde{\chi}} h^2$ as above, and satisfies all other phenomenological constraints. In addition we have shaded (light red) the regions excluded by collider limits and by $\Omega_{\tilde{\chi}} h^2 > 0.13$.⁶

In Fig. 2 we present a more detailed analysis of the same $m_{16} = 3 \text{ TeV}$, $m_A = 500 \text{ GeV}$ case given in Fig. 1. We now include lines of constant BR ($B_s \rightarrow \tilde{\chi}^+ \tilde{\chi}^-$) (upper left), m_h (upper right), $\Omega_{\tilde{\chi}} h^2$ (lower left), and $\sigma_{\text{SI}}^{\text{SI}}$ (lower right). $\sigma_{\text{SI}}^{\text{SI}}$ is the spin independent neutralino dark matter cross-section relevant for direct dark matter searches. We now consider each one of these features further.

⁶A similar analysis was performed in the recent paper [4]. However, they were not able to find acceptable cosmological solutions. It appears that they did not find any acceptable solutions because they found Yukawa unification only for $M_{1/2} \approx 100 \text{ GeV}$ and large $\tan\beta > 300$. In this region we probably would not find acceptable solutions for $\Omega_{\tilde{\chi}} h^2$, no matter what value we take for m_A .

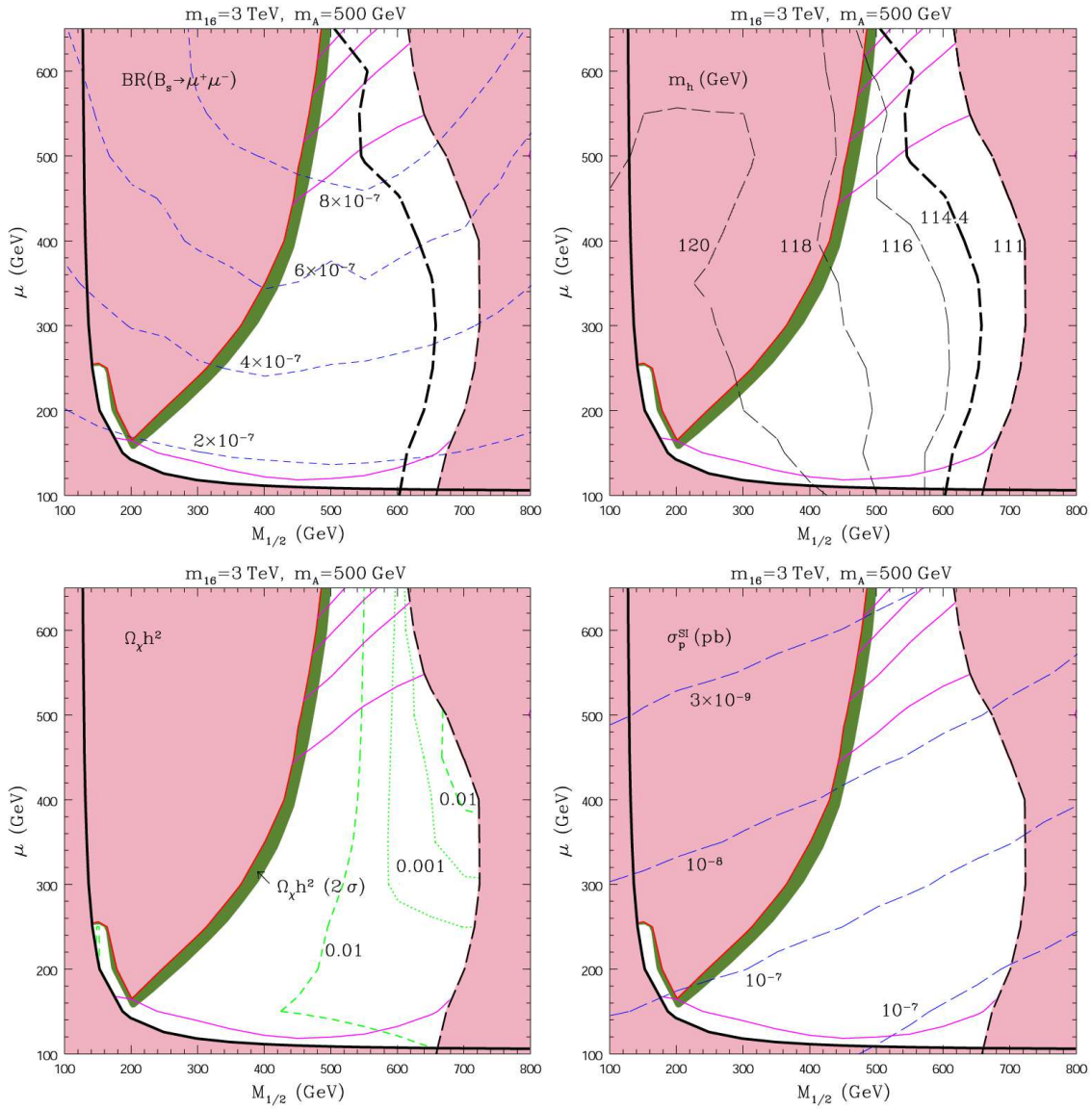


Figure 2: Same as Fig. 1 with contours of constant $BR(B_s \rightarrow \mu^+ \mu^-)$ (upper left), m_h (upper right), $\Omega_\chi h^2$ (lower left) and σ_p^{SI} (lower right) for $m_{16} = 3$ TeV and $m_A = 500$ GeV.

Recall, the branching ratio $BR(B_s \rightarrow \mu^+ \mu^-)$ is sensitive to the value of the CP odd Higgs mass m_A [7]. For $m_A = 500$ GeV, the branching ratio satisfies $2 \times 10^{-7} < BR(B_s \rightarrow \mu^+ \mu^-) < 8 \times 10^{-7}$ for acceptable values of h^2 and $2 < \Omega_\chi h^2$. In a recent analysis it has been shown that, with an integrated luminosity of 15 fb^{-1} , CDF can discover this process if $BR(B_s \rightarrow \mu^+ \mu^-) > 1.2 \times 10^{-8}$ [22]. Hence most acceptable regions of parameter space lead to observable rates for $BR(B_s \rightarrow \mu^+ \mu^-)$.

In Fig. 2 (upper right) we see that the light Higgs mass increases as $M_{1/2}$ decreases. In the acceptable regions of parameter space we find $116 < m_h < 121$ GeV. The value of the light Higgs mass is however fairly insensitive to m_{16} .

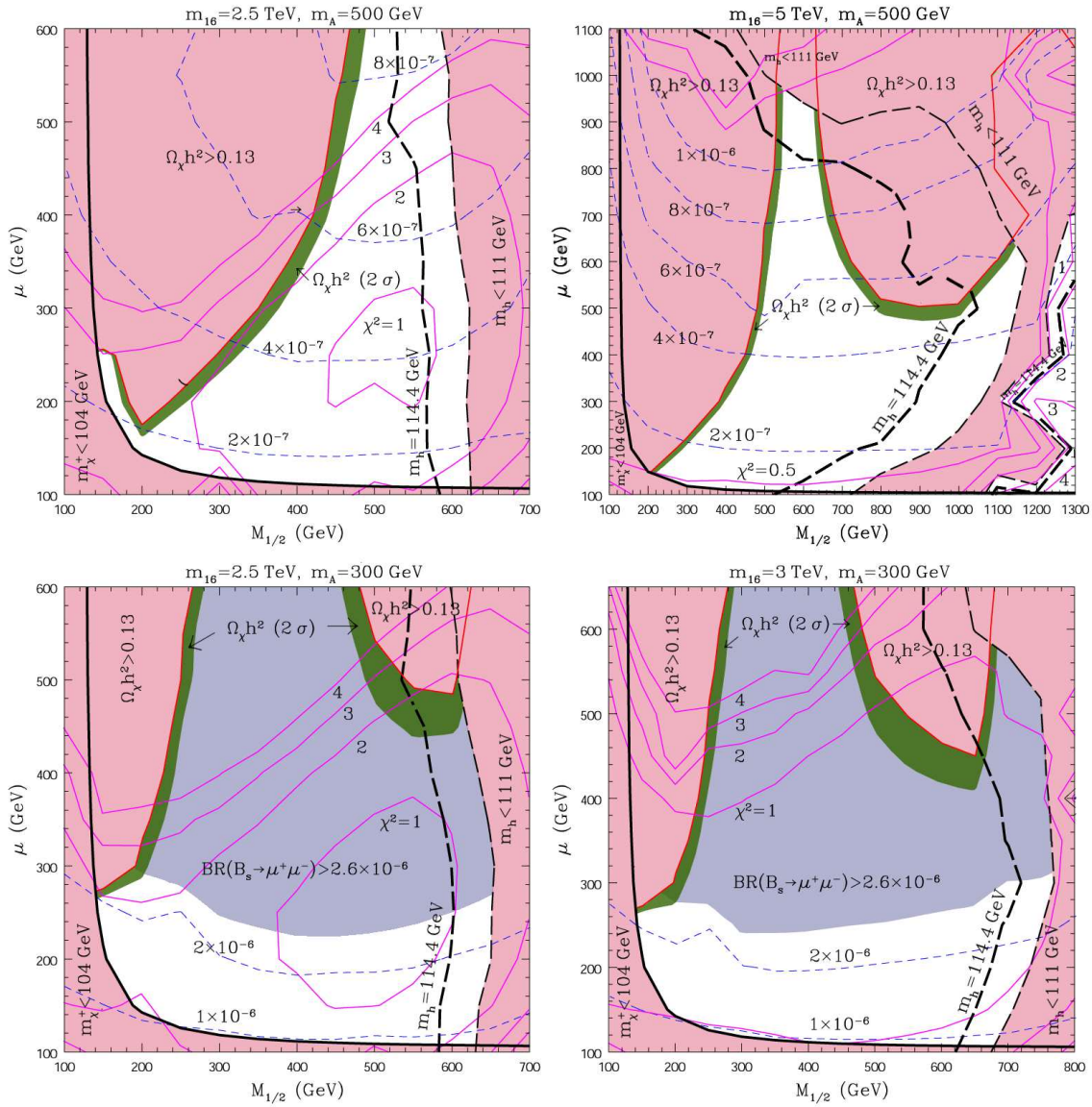


Figure 3: The same as in Fig.1 but for $m_{16} = 2.5$ TeV and $m_A = 500$ GeV (upper left), $m_{16} = 5$ TeV and $m_A = 500$ GeV (upper right), $m_{16} = 2.5$ TeV and $m_A = 300$ GeV (lower left) and $m_{16} = 3$ TeV and $m_A = 300$ GeV (lower right). Also marked are contours of constant $BR(B_s \rightarrow \mu^+ \mu^-)$. The blue regions in the lower two panels are excluded by $BR(B_s \rightarrow \mu^+ \mu^-) > 2.6 \times 10^{-6}$. Note the different mass ranges for $M_{1/2}$ and μ in the different panels.

The cosmological relic abundance of the neutralino h^2 (Fig. 2 (lower left)) is primarily determined by the direct s-channel pair annihilation into SM fermion pairs through the CP odd Higgs. Since all the sfermions are very heavy, their contribution to reducing the neutralino number density is strongly suppressed. In contrast, because of the coupling $A_{bb} / \tan \beta$ (and similarly for the 's), the A resonance is effective and broad. Near $m_{16} = m_A = 2$ it reduces h^2 down to allowed but uninterestingly small values 0.1 . As one moves away from the resonance, h^2 grows, reaches the preferred range

$0.095 < h^2 < 0.13$, before becoming too large $h^2 > 0.13$.⁷ (A similar, but much more narrow resonance due to h^0 is also present at $M_{1=2} \approx 150$ GeV and small μ .) When $m_A > m_t$ ($M_{1=2} > 420$ GeV) and the stops are not too heavy, the LSP pairs annihilate to $t\bar{t}$ pairs. In the region of large $M_{1=2}$, often where m_h is already too low, two additional channels become effective. First, in this region the neutralino becomes almost mass degenerate with the lighter stau which leads to reducing h^2 through coannihilation. Second, if m_A is not too large, neutralino pair annihilation into Higgs boson pairs AA and HH opens up. Finally, at $M_{1=2}$, the relic abundance is strongly reduced due to the increasing higgsino component of the LSP.

Finally, the spin independent neutralino cross section σ_p^{SI} in the lower right window of Fig. 2 is predominantly determined by the contribution of the heavy CP even scalar (channel exchange to both tree level and one loop diagrams. Note that in the preferred region of $\mu^2 < 2$ and $0.095 < h^2 < 0.13$ we find 10^{-9} pb $< \sigma_p^{SI} < 10^{-7}$ pb. We will comment further on our predictions for σ_p^{SI} below.

In Fig. 3 we display the dependence of our constraints, h^2 and $BR(B_s \rightarrow \tau^+ \tau^-)$ on m_{16} and m_A . By comparing the upper two windows with Fig. 1 we can see that, as m_{16} increases, the region with $\mu^2 < 2$ rapidly grows. Note, the dominant pull in μ^2 is due to the bottom quark mass. In order to fit the data, the total SUSY corrections to m_b (m_b) must be of order $(2-4)\%$ [2]. In addition there are three dominant contributions to these SUSY corrections, a gluino loop contribution $\propto M_g \tan \beta = m_{\tilde{b}_1}^2$, a chargino loop contribution $\propto \frac{2}{t} A_t \tan \beta = m_{\tilde{t}_1}^2$, and a term $\propto \log M_{SUSY}^2$. When m_{16} increases (with $M_{1=2}$ fixed) the parameter A_t becomes more negative, since $A_0 \approx 2 m_{16}$ and $A_t \approx 3 M_{1=2} + A_0$ where $\mu^2 < 1$. Also, larger values of m_{16} permit a larger range for the ratio $m_{\tilde{b}_1} = m_{\tilde{t}_1}$. Thus larger values of m_{16} allow more freedom in parameter space for fitting the data at both smaller or larger values of μ^2 ; $M_{1=2}$.

In the lower two windows in Fig. 3 we consider two regions with $m_A = 300$ GeV with $m_{16} = 2.5$ TeV (lower left) and $m_{16} = 3$ TeV (lower right). The blue regions are excluded by the CDF bound $BR(B_s \rightarrow \tau^+ \tau^-) < 2.6 \cdot 10^{-6}$ [8]. Note for $m_{16} = 2.5$ TeV, the region with $\mu^2 < 2$ does not overlap the region with acceptable dark matter abundance (green shaded). However for $m_{16} = 3$ TeV, $m_A = 300$ GeV, Fig. 3 (lower right), we find a small region with acceptable $\mu^2 < 1$ and h^2 . Moreover the branching ratio $BR(B_s \rightarrow \tau^+ \tau^-)$ is now close to the CDF bound. On the other hand for $m_{16} = 5$ TeV, $m_A = 500$ GeV, in Fig. 3 (upper right), a new region of parameter space consistent with all the data now opens up with larger μ^2 ; $M_{1=2}$. This new region becomes cosmologically allowed due to neutralino annihilation into Higgs boson pairs AA and HH and due to coannihilation with the lighter stau.

Hence we see that increasing m_A has two effects. It suppresses the branching fraction $BR(B_s \rightarrow \tau^+ \tau^-)$. At the same time it moves the s-channel neutralino annihilation channel to larger values of $M_{1=2}$; hence providing larger regions with $0.095 < h^2 < 0.13$ (compare Figs. 1 and 3 (lower right) or Figs. 3 (upper and lower left)). In fact, the two

⁷Note that at one loop we have $M_1(M_Z) = M_{1=2} - \frac{1}{2} M_Z = g$ so $M_1(M_Z) \approx 0.4 M_{1=2}$. For binos (like neutralino (which is true for larger μ), we thus have $m_0 \approx 0.4 M_{1=2}$. Hence for s-channel annihilation we have $m_A \approx 2m_0 \approx 0.8 M_{1=2}$ or $M_{1=2} \approx (5/4) m_A$ for the position of the peak suppression."

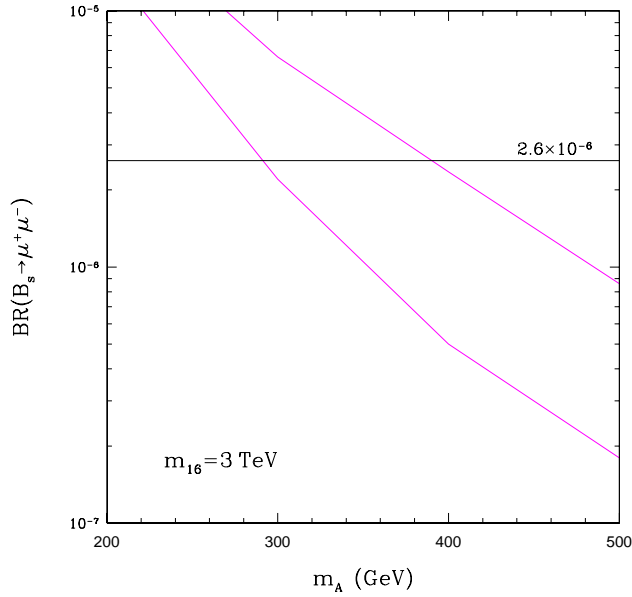


Figure 4: The upper and lower limits on $BR(B_s \rightarrow \mu^+ \mu^-)$ as a function of m_A in the $\tilde{\chi}_{1=2}$ region of parameter space satisfying all the collider constraints, $0.095 < h^2 < 0.13$ and $\tan^2 \beta < 2$ for fixed $m_{16} = 3 \text{ TeV}$.

(green) branches of the preferred range $0.095 < h^2 < 0.13$ correspond to the two sides (except for the upper left window of Fig. 3 where just one side is evident) of the wide A resonance in the neutralino pair-annihilation. On the other hand, increasing m_A above 1 TeV or so would move the regions of preferred h^2 too far to the right, in potential conflict with a lower bound on m_h .

Finally, we comment on $BR(B \rightarrow X_s \gamma)$. The current experimental range [23, 24] is $BR(B \rightarrow X_s \gamma)_{\text{expt}} = (3.41 - 0.36) \cdot 10^4$, while the SM prediction, including full NLO QCD corrections [25, 26], is $BR(B \rightarrow X_s \gamma)_{\text{SM}} = (3.70 - 0.30) \cdot 10^4$. In computing the SUSY contribution to $b \rightarrow s \gamma$ we further include full LO and dominant NLO level $\tan \beta$ enhanced contributions [27, 28]. Conservatively allowing for the SM + SUSY contribution to be in the range $(3.41 - 0.67) \cdot 10^4$ [29, 24] selects a band $300 \text{ GeV} < m_A < 400 \text{ GeV}$ which slowly decreases with increasing $M_{1=2}$. (This remains approximately true for all the cases that we have analyzed except $m_{16} = 5 \text{ TeV}$ and $m_A = 500 \text{ GeV}$ where one finds a narrower range at $m_A < 200 \text{ GeV}$.) However, $BR(B \rightarrow X_s \gamma)$ is strongly sensitive to the 2{3 generation down-type squark mixings [24] which are model dependent and which we do not include here. In summary, the process is generally consistent with the most preferred regions of $M_{1=2}$ and m_A but we do not use it here as a constraint, since it can be easily relaxed by employing parameters which are less relevant for our analysis.

To summarize, we find that regions satisfying all three constraints exist for $m_{16} \approx 3 \text{ TeV}$ and $m_A \approx 300 \text{ GeV}$. The acceptable range for $\tilde{\chi}_{1=2}$ grows with increasing m_A

(for fixed $m_{16} = 3 \text{ TeV}$) from approximately 260 GeV to 295 GeV , 140 GeV to 200 GeV for $m_A = 300 \text{ GeV}$ to 160 GeV and 520 GeV , 140 GeV to 530 GeV for $m_A = 500 \text{ GeV}$. In addition, the allowed regions grow as m_{16} increases and for $m_A = 500 \text{ GeV}$; $m_{16} = 5 \text{ TeV}$ there is also a large $\tilde{M}_{1=2}$ solution satisfying 480 GeV to 820 GeV ; 640 GeV to 1020 GeV . In the Table we present the input and output data from the χ^2 analysis for three points satisfying all the phenomenological constraints.

4. Predictions and Summary

In this paper we have analyzed the $M_{SO_{10}SM}$ and found regions of soft SUSY breaking parameter space which fit precision electroweak data, including the top, bottom and tau masses and, in addition, fit the cosmological dark matter abundance for the neutralino LSP and satisfy $BR(B_s \rightarrow \tau^+ \nu)$. Generically, we find solutions to all the constraints with $m_{16} \geq 3 \text{ TeV}$. The squark and slepton masses have an inverted scalar mass hierarchy with the first and second generation scalar masses of order m_{16} , while the third generation has mass less than 1.3 TeV for $m_{16} = 5 \text{ TeV}$. This nice feature of the model suppresses SUSY CP and flavor problems. In addition the gaugino masses are typically much lighter, except for the large $\tilde{M}_{1=2}$ region for $m_{16} = 5 \text{ TeV}$ with a gluino mass of order 1.7 TeV (see spectrum in Table for selected acceptable points).

Note an immediate consequence of such heavy first and second generation sleptons is the suppression of the SUSY contribution to the anomalous magnetic moment of the muon. We find $a^{\text{SUSY}}_{\mu} \approx 2.8 \times 10^{-10}$ (see Table). This is consistent with the most recent experimental [30] and theoretical results at 1 σ if one uses χ^2 based analysis [31]. However it is only consistent with an e^+e^- based analysis at 3σ .

Another interesting result is the enhanced branching ratio for the process $B_s \rightarrow \tau^+ \nu$. In Fig. 4 we show the ranges of values of $BR(B_s \rightarrow \tau^+ \nu)$ in the low $\tilde{M}_{1=2}$ region of parameter space satisfying all the phenomenological constraints with $0.095 < h^2 < 0.13$ and $\tan^2 \beta < 2$ as a function of m_A for fixed $m_{16} = 3 \text{ TeV}$. The horizontal red line is the CDF bound. Over a significant region of parameter space $BR(B_s \rightarrow \tau^+ \nu) > 1 \times 10^{-7}$ and may be observable at the Tevatron (Run II) [22].

Finally in Fig. 5 we present the cross-section for elastic neutralino-proton scattering due to scalar interactions σ_p^{SI} for all regions satisfying the collider constraints, $0.095 < h^2 < 0.13$ and $\tan^2 \beta < 2$. The green bands are for $m_{16} = 2.5 \text{ TeV}$, the red for 3 TeV and the blue for 5 TeV . The lighter shading is for $m_A = 300 \text{ GeV}$, the darker for $m_A = 500 \text{ GeV}$. In the last case ($m_{16} = 5 \text{ TeV}$ and $m_A = 500 \text{ GeV}$) there are two branches which correspond to the two cosmologically preferred regions in the upper right panel in Fig. 3. Note that lower m_A generally gives larger σ_p^{SI} as expected. For comparison, we also show the bounds from the present dark matter searches and the predictions of the general MSSM [32]. (Other recent studies of σ_p^{SI} in the case of non-universal Higgs mass in a variant of the CMSSM can be found in [33].) Over the next two to five years the experimental sensitivity is expected to gradually improve by some three orders of magnitude. This will cover large

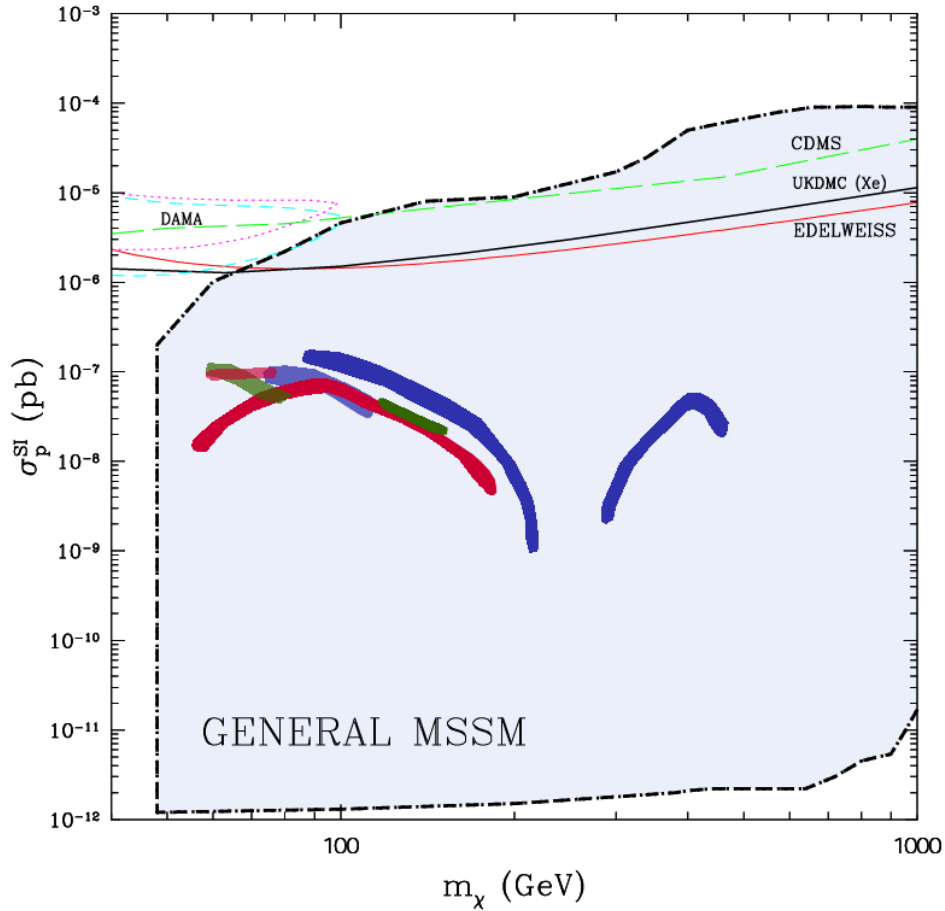


Figure 5: Predictions for σ_p^{SI} vs. m_χ for different choices of m_{16} and m_A , subject to the collider constraints, $0.095 < h^2 < 0.13$ and $\Omega_\chi^2 < 3$. The green bands are for $m_{16} = 2.5$ TeV, the red for 3 TeV and the blue for 5 TeV. The lighter shading is for $m_A = 300$ GeV, the darker for $m_A = 500$ GeV. In the last case ($m_{16} = 5$ TeV and $m_A = 500$ GeV) there are two branches which correspond to the two cosmologically preferred regions in the upper right panel in Fig. 3.

parts of the predicted ranges of σ_p^{SI} , especially at lower values of m_A where $B_S \rightarrow \pi^+ \pi^0$ will be accessible at the Tevatron (Run II).

Acknowledgments

We gratefully acknowledge the use of the GUT Ω_χ^2 analysis code developed by T. Blazek and a contribution from Y.G.Kim to a routine for computing $BR(B_S \rightarrow \pi^+ \pi^0)$. L.R. is grateful to A. Melchiorri for helpful comments regarding the recent WMAP analysis. R.D. is supported, in part, by the U.S. Department of Energy, Contract DE-FG 03-91ER-40674 and the Davis Institute for High Energy Physics. S.R. received partial support from DOE grant# DOE/ER/01545-841 and from a grant in aid from the Monell Foundation. He is also grateful to the hospitality shown to him by the School of Natural Sciences, Institute

for Advanced Study. RRdA and LR are supported in part by the EU Fifth Framework network "Supersymmetry and the Early Universe" (HPRN-CT-2000-00152).

References

- [1] G.L. Kane, C.F. Kolda, L. Roszkowski and J.D. Wells, Phys. Rev. D 49, 6173 (1994) [[arXiv:hep-ph/9312272](#)].
- [2] T. Blazek, R. Dermisek and S. Raby, Phys. Rev. Lett. 88, 111804 (2002) [[arXiv:hep-ph/0107097](#)]; Phys. Rev. D 65, 115004 (2002) [[arXiv:hep-ph/0201081](#)].
- [3] K. Tobe and J.D. Wells, [[arXiv:hep-ph/0301015](#)].
- [4] D. Auto, H. Baer, C. Balazs, A. Belyaev, J. Ferrandis and X. Tata, [[arXiv:hep-ph/0302155](#)].
- [5] M. Olechowski and S. Pokorski, Phys. Lett. B 344, 201 (1995) [[arXiv:hep-ph/9407404](#)]; D. M. Ataliotakis and H. P. Nilles, Nucl. Phys. B 435, 115 (1995) [[arXiv:hep-ph/9407251](#)]; N. Polonsky and A. Pomarol, Phys. Rev. D 51, 6532 (1995) [[arXiv:hep-ph/9410231](#)]; H. Murayama, M. Olechowski and S. Pokorski, Phys. Lett. B 371, 57 (1996) [[arXiv:hep-ph/9510327](#)]; R. Rattazzi and U. Sarid, Phys. Rev. D 53, 1553 (1996) [[arXiv:hep-ph/9505428](#)].
- [6] See, e.g., latest WMAP results in D. N. Spergel et al., [[arXiv:astro-ph/0302209](#)].
- [7] G. Isidori and A. Retico, JHEP 0111, 001 (2001) [[arXiv:hep-ph/0110121](#)]; A. Dedes, H. K. Dreiner and U. Nierste, Phys. Rev. Lett. 87, 251804 (2001) [[arXiv:hep-ph/0108037](#)]; K. S. Babu and C. F. Kolda, Phys. Rev. Lett. 84, 228 (2000) [[arXiv:hep-ph/9909476](#)] and references therein.
- [8] F. Abe et al. [CDF Collaboration], Phys. Rev. D 57, 3811 (1998).
- [9] J. A. Bagger, J. L. Feng, N. Polonsky and R. J. Zhang, Phys. Lett. B 473, 264 (2000) [[arXiv:hep-ph/9911255](#)].
- [10] F. Gabbiani, E. Gabrielli, A. Masiero and L. Silvestrini, Nucl. Phys. B 477, 321 (1996) [[arXiv:hep-ph/9604387](#)]; T. Besmer, C. Greub, and T. Hurth, Nucl. Phys. B 609, 359 (2001) [[arXiv:hep-ph/0105292](#)].
- [11] E. Keams, Snowmass 2001, <http://hep.bu.edu/>
- [12] R. Dermisek, A. Ma and S. Raby, Phys. Rev. D 63, 035001 (2001) [[arXiv:hep-ph/0007213](#)].
- [13] T. Blazek, M. Carena, S. Raby and C. E. Wagner, Phys. Rev. D 56, 6919 (1997) [[arXiv:hep-ph/9611217](#)].
- [14] H. E. Haber and R. Hemping, Phys. Rev. D 48, 4280 (1993) [[arXiv:hep-ph/9307201](#)]; M. Carena, J. R. Espinosa, M. Quiros and C. E. Wagner, Phys. Lett. B 355, 209 (1995) [[arXiv:hep-ph/9504316](#)]; M. Carena, M. Quiros and C. E. Wagner, Nucl. Phys. B 461, 407 (1996) [[arXiv:hep-ph/9508343](#)].
- [15] The Review of Particle Physics, D. E. Groom, et al., The European Physical Journal C 15, 1 (2000).
- [16] M. Beneke and A. Signer, Phys. Lett. B 471, 233 (1999) [[arXiv:hep-ph/9906475](#)].
G. Corcella and A. H. Hoang, Phys. Lett. B 554, 133 (2003) [[arXiv:hep-ph/0212297](#)].
- [17] P. Langacker, talk at Chicagoland seminar, October (1999).

- [18] T. N. Ihei, L. Roszkowski and R. Ruiz de Austri, JHEP 0105, 063 (2001) [[arXiv:hep-ph/0102308](#)]; JHEP 0203, 031 (2002) [[arXiv:hep-ph/0202009](#)].
- [19] J. Edsjö and P. Gondolo, Phys. Rev. D 56, 1879 (1997) [[arXiv:hep-ph/9704361](#)].
- [20] T. N. Ihei, L. Roszkowski and R. Ruiz de Austri, JHEP 0207, 024 (2002) [[arXiv:hep-ph/0206266](#)].
- [21] P. Gondolo, J. Edsjö, L. Bergstrom, P. Ullio, and T. Baltz, <http://www.physto.se/edsjo/darksusy/>.
- [22] R. Amositt, B. Dutta, T. Kamon and M. Tanaka, Phys. Lett. B 538, 121 (2002) [[arXiv:hep-ph/0203069](#)].
- [23] S. Chen, et al. [CLEO Collaboration], Phys. Rev. Lett. 87, 251807 (2001) [[arXiv:hep-ex/0108032](#)]; R. Barate, et al. [ALEPH Collaboration], Phys. Lett. B 429, 169 (1998); K. Abe, et al. [Belle Collaboration], Phys. Lett. B 511, 151 (2001) [[arXiv:hep-ex/0103042](#)]; C. Jessop, et al. [BaBar Collaboration], talk at ICHEP {02, Amsterdam, July, 2002.
- [24] K. Okumura and L. Roszkowski, [[arXiv:hep-ph/0208101](#)].
- [25] P. Gambino and M. Misiak, Nucl. Phys. B 611, 338 (2001) [[arXiv:hep-ph/0104034](#)].
- [26] A. J. Buras, A. Czarnecki, M. Misiak and J. Urban, Nucl. Phys. B 631, 219 (2002) [[arXiv:hep-ph/0203135](#)], and reference therein.
- [27] G. Degrassi, P. Gambino and G. F. Giudice, JHEP 0012, 009 (2000) [[arXiv:hep-ph/0009337](#)].
- [28] M. Carena, D. Garcia, U. Nierste and C. E. Wagner, Phys. Lett. B 499, 141 (2001) [[arXiv:hep-ph/0010003](#)].
- [29] L. Roszkowski, R. Ruiz de Austri and T. N. Ihei, JHEP 0108, 024 (2001) [[arXiv:hep-ph/0106334](#)].
- [30] G. W. Bennett et al. [Muon g-2 Collaboration], Phys. Rev. Lett. 89, 101804 (2002) [Erratum {*ibid.* 89, 129903 (2002)}] [[arXiv:hep-ex/0208001](#)].
- [31] M. Davier, S. Eidelman, A. Hocker and Z. Zhang, [[arXiv:hep-ph/0208177](#)].
- [32] Y. G. Kim, T. N. Ihei, L. Roszkowski and R. Ruiz de Austri, J. High Energy Phys. 0212 (034) 2002, [[arXiv:hep-ph/0208069](#)].
- [33] For recent analyses see, e.g., J. Ellis, A. Ferstl, K. A. Olive, Y. Santoso, [[arXiv:hep-ph/0302032](#)]; V. Bertin, E. Nezri, J. Orloff, [[arXiv:hep-ph/0210034](#)].

Data points		1	2	3
Input parameters				
G^1 $M_G \cdot 10^{16}$ μ		24:66 3:51 0:038 0:66	24:92 2:83 0:034 0:66	25:28 2:43 0:029 0:66
m_{16} $m_{10} = m_{16}$ m_H^2 $M_{1=2}$ $\tan\beta$ $A_0 = m_{16}$		3000 1:30 0:14 180 270 50:9 1:85	3000 1:33 0:15 400 350 50:6 1:88	5000 1:33 0:14 700 600 50:5 1:91
2 observables	Exp ()			
M_Z M_W $G \cdot 10^5$ μ_{EM}^1 $\mu_s(M_Z)$ $\mu_{new} \cdot 10^3$	91:188 (0:091) 80:419 (0:080) 1:1664 (0:0012) 137:04 (0:14) 0:118 (0:002) 0:200 (1:10)	91:18 80:42 1:166 137:0 0:1177 0:427	91:19 80:42 1:166 137:0 0:1176 0:498	91:20 80:41 1:166 137:0 0:1179 0:162
M_t $m_b(m_b)$ M	174:3 (5:1) 4:20 (0:20) 1:7770 (0:0018)	173:9 4:28 1:777	174:7 4:28 1:777	174:7 4:21 1:777
TOTAL 2		0:53	0:61	0:13
h H A H^+ μ_0 μ_1 μ_2 μ_+ μ_1 μ μ_1 μ_1 μ_1		120 329 299 329 72 133 133 474 300 679 870	119 556 499 540 163 288 287 1032 300 736 721	117 557 501 541 293 536 535 1768 576 1262 1180
$a^{SUSY} \cdot 10^{10}$ h^2 $\sigma_p^{SI}(\text{pb}) \cdot 10^7$ $BR(B_s \rightarrow X_s \gamma) \cdot 10^6$ $BR(B \rightarrow X_s \gamma) \cdot 10^4$	25:6 (16) 0:095 0:130 < 2:6 3:41 (0:67)	2:7 0:099 1:020 2:58 5:36	2:8 0:130 0:158 0:61 4:34	1:0 0:097 0:049 0:66 0:81